

Quasi-one-dimensional solutions for domain walls and their constraints in improper ferroelastics

Wenwu Cao

*Materials Research Laboratory and Department of Physics, Pennsylvania State University,
University Park, Pennsylvania 16802
and Laboratory of Atomic and Solid State Physics, Cornell University, Ithaca, New York 14853-2501*

Gerhard R. Barsch

*Materials Research Laboratory and Department of Physics, Pennsylvania State University,
University Park, Pennsylvania 16802*

James A. Krumhansl

*Laboratory of Atomic and Solid State Physics, Cornell University, Ithaca, New York 14853-2501
(Received 21 May 1990)*

Based on a Landau-Ginzburg model for improper ferroelastic perovskites, we have analyzed quasi-one-dimensional (Q1D) solutions for twin boundaries (domain walls) and the associated constraints. Because of the coupling of the order parameter to the elastic strain, in general domain walls must be described by fully three-dimensional (3D) solutions. Q1D solutions exist only with the presence of one of the following: (i) body force, (ii) surface stress, and (iii) interface dislocations. The shape change induced by the domain wall is also discussed for each of the above three cases. These conclusions hold quite generally for all Landau-Ginzburg models of improper ferroelastics.

I. INTRODUCTION

Previous models of planar interphase boundaries are based on the assumption that they have quasi-one-dimensional (Q1D) nature.¹⁻¹³ While this may be justified in some disordered system, such as liquid vapor, etc., it is not always true for a solid system with definite structural symmetry. As pointed out in our previous paper¹⁴ the existence of Q1D solutions (in a 3D solid) for coherent interphase (twin and antiphase) boundaries (without interface dislocations) requires lateral surface stresses. That result is, as we will see later, due to the 3D nature of solids rather than an artifact of a particular model. In fact, for all improper ferroelastic systems, the Q1D reduction can be attained only under certain mechanical constraints when strain coupling is included; the Poisson contraction, which is an intrinsic feature of solids, correlates the dimensional changes along different spatial directions. In this paper we will address these constraints in connection with Q1D solutions for domain walls in solids, and in addition describe the induced shape change for a particular example of an improper ferroelastic system. The coupling between order parameter and elastic strain is important to properly interpret experimental results, because the boundary conditions imposed (e.g., by the sample holder) could produce substantial effects.

The *Basic Assumption* underlying Q1D solutions is the following: *All physical quantities are invariant under translations parallel to the planar domain wall.* With this assumption one can choose the independent variable to be in the direction normal to the domain wall, thus rendering a problem quasi-one-dimensional. However, if the elastic continuity requirement is imposed this as-

sumption is only conditionally justified, especially when close to a domain wall.

In order to state this problem more clearly, we analyze a particular example: the analytic solutions that describe the 90° domain walls (twin boundaries) between the tetragonal variants in an improper ferroelastic perovskite system.¹⁴ Although these analytic solutions correspond to a special choice of parameters, the conclusions drawn here are general, and should be applicable to all two- and three-dimensional improper ferroelastics, including ferromagnetic, ferroelectric and superconducting systems, etc., when the coupling of primary order parameter to elastic strain is not negligible.

The contents of this paper are as follows: in Sec. II we briefly introduce the model to be used, in Sec. III we discuss the Q1D solutions and the associated constraints, including the shape change induced by each solution. The final section contains the summary and conclusions.

II. THE MODEL

We consider the $O_h^1-D_{4h}^{18}$ ($Pm\bar{3}m-I4/mcm$) improper ferroelastic phase transition in perovskites (ABX_3), which is characterized by the rotation of the BX_6 octahedra. We take directly from our previous paper (Ref. 14) the free-energy expansion, which is an extension of the Landau theory developed by Slonczewski and Thomas¹⁵ to include the order-parameter gradient energy F_g ,

$$F = F_L(Q_i) + F_{el}(u_{k,l}) + F_c(Q_i, u_{k,l}) + F_g(Q_{i,j}), \quad (1a)$$

$$F_L(Q_i) = \frac{1}{2}K(Q_1^2 + Q_2^2 + Q_3^2) + A(Q_1^2 + Q_2^2 + Q_3^2)^2 + A_n(Q_1^2Q_2^2 + Q_1^2Q_3^2 + Q_2^2Q_3^2), \quad (1b)$$

$$F_{el}(u_{k,l}) = \frac{1}{2}c_{11}(\eta_{11}^2 + \eta_{22}^2 + \eta_{33}^2) + c_{12}(\eta_{11}\eta_{22} + \eta_{11}\eta_{33} + \eta_{22}\eta_{33}) + 2c_{44}(\eta_{12}^2 + \eta_{13}^2 + \eta_{23}^2), \quad (1c)$$

$$F_c(Q_i, u_{k,l}) = -B_1(\eta_{11}Q_1^2 + \eta_{22}Q_2^2 + \eta_{33}Q_3^2) - 2B_t(\eta_{12}Q_1Q_2 + \eta_{13}Q_1Q_3 + \eta_{23}Q_2Q_3) - B_2[\eta_{11}(Q_2^2 + Q_3^2) + \eta_{22}(Q_1^2 + Q_3^2) + \eta_{33}(Q_1^2 + Q_2^2)], \quad (1d)$$

$$F_g(Q_{i,j}) = \frac{1}{2}D_{11}(Q_{1,1}^2 + Q_{2,2}^2 + Q_{3,3}^2) + D_{12}(Q_{1,1}Q_{2,2} + Q_{1,1}Q_{3,3} + Q_{2,2}Q_{3,3}) + \frac{1}{2}D_{44}[(Q_{1,2} + Q_{2,1})^2 + (Q_{1,3} + Q_{3,1})^2 + (Q_{2,3} + Q_{3,2})^2]. \quad (1e)$$

Here $Q_i = \frac{1}{2}a \tan \phi_i$ ($i = 1, 2, 3$; a is the lattice constant), representing the rotation of the BX_6 octahedra,¹⁵ is the primary order parameter; u_i is the component of the elastic displacement field and

$$\eta_{ij} = \frac{1}{2}(u_{i,j} + u_{j,i})$$

are the components of the linearized strain tensor which serves as a secondary order parameter.

Since we are seeking Q1D solutions of the form $Q(s)$ and $\tilde{\eta}(s)$, where $s = \mathbf{x} \cdot \hat{\mathbf{n}}$ and $\hat{\mathbf{n}}$ is the unit vector along $[\bar{1}10]$, it is convenient to work in the r - s coordinate system which is obtained by rotation of the crystallographic axes by 45° around $[001]$.

There are two coupled fields: the order parameter Q represents the ion motion within a unit cell ("shuffle"), and $\tilde{\eta}$ describes the elastic distortion of a unit cell. The static equilibrium conditions for Q and $\tilde{\eta}$ are given by Euler's equation. In addition, the elastic compatibility relations must be satisfied by the strain components for a defect-free domain wall. Therefore, we have the following equations:

$$\frac{\partial}{\partial x_j} \frac{\partial F}{\partial Q_{i,j}} - \frac{\partial F}{\partial Q_i} = 0, \quad (2)$$

$$\sigma_{ij,j}^{\text{tot}} = \frac{\partial}{\partial x_j} \left[\frac{\partial F}{\partial \eta_{ij}} \right] = 0, \quad (3)$$

$$\epsilon_{ikl} \epsilon_{jmn} \eta_{ln,km} = 0. \quad (4)$$

In the new coordinates, $i, j, k, l, m, n = r, s, x_3$; σ^{tot} is the total stress tensor and ϵ_{ikl} is the totally antisymmetric Levi-Civita tensor.

Under the basic assumption there are only three non-trivial constraints from Eq. (4),

$$\eta_{rr,ss} = 0, \quad (5a)$$

$$\eta_{33,ss} = 0, \quad (5b)$$

$$\eta_{r3,ss} = 0. \quad (5c)$$

The boundary conditions at $s = \pm \infty$ are determined by the physical requirement that the order parameter and

strain components of the twin crystal must have the values corresponding to one of the low-temperature variants, i.e.,¹⁴

$$\lim_{s \rightarrow \pm \infty} Q_r = Q_0 / \sqrt{2}, \quad (6a)$$

$$\lim_{s \rightarrow \pm \infty} Q_s = \pm Q_0 / \sqrt{2}, \quad (6b)$$

$$\lim_{r \rightarrow \pm \infty} \eta_{rr} = \lim_{s \rightarrow \pm \infty} \eta_{ss} \quad (6c)$$

$$= (\eta_{\parallel} + \eta_{\perp}) / 2, \quad (6d)$$

$$\lim_{s \rightarrow \pm \infty} \eta_{rs} = \pm (\eta_{\parallel} - \eta_{\perp}) / 2, \quad (6e)$$

where

$$Q_0 = (-K/4A')^{1/2}, \quad (7a)$$

$$A' = A - \frac{\hat{B}_{11}^2}{6\hat{c}_{11}} - \frac{\hat{B}_{22}^2}{3\hat{c}_{22}}, \quad (7b)$$

$$\hat{B}_{11} = B_1 + 2B_2, \quad (8a)$$

$$\hat{B}_{22} = B_1 - B_2, \quad (8b)$$

$$\hat{c}_{11} = c_{11} + 2c_{12}, \quad (8c)$$

$$\hat{c}_{22} = c_{11} - c_{12}, \quad (8d)$$

$$\eta_{\parallel} = \frac{Q_0^2}{3} \left[\frac{\hat{B}_{11}}{\hat{c}_{11}} + \frac{2\hat{B}_{22}}{\hat{c}_{22}} \right], \quad (9a)$$

$$\eta_{\perp} = \frac{Q_0^2}{3} \left[\frac{\hat{B}_{11}}{\hat{c}_{11}} - \frac{\hat{B}_{22}}{\hat{c}_{22}} \right]. \quad (9b)$$

Q_0 , η_{\parallel} , and η_{\perp} are the values for the order parameter and for the strain components parallel and perpendicular to the tetragonal axis, respectively, in the low-temperature phase of a homogeneous system.^{14,15}

III. ANALYTIC Q1D SOLUTIONS FOR $[\bar{1}10]$ DOMAIN WALL

A twinned low-temperature structure can be formed as follows (see Fig. 1). First, imagine making a cut along the dashed line in the cubic phase; second, transform the system so that in the left half the tetragonal axis is $[100]$, but for the right half is $[010]$, then finally join the two transformed pieces together. There are no interface de-

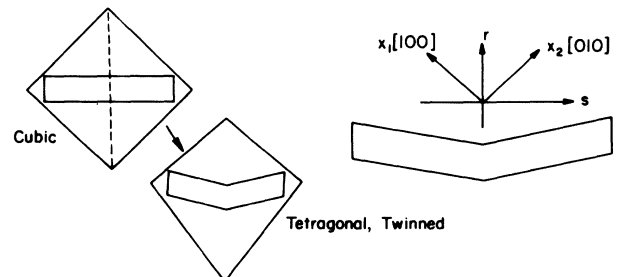


FIG. 1. Bending associated with the formation of a twin boundary and the coordinate systems used in this paper; x_3 is directed into the page away from the reader.

fects generated in the process, i.e., no atoms were lost or gained. However, the so formed twin boundary is discontinuous and the nonzero strain components are

$$\eta_{rr} = \eta_{ss} \quad (10a)$$

$$= \frac{1}{2}(\eta_{\parallel} + \eta_{\perp}), \quad (10b)$$

$$\eta_{rs} = \frac{1}{2}(\eta_{\parallel} - \eta_{\perp})[\theta(s) - \theta(-s)], \quad (10c)$$

$$\eta_{33} = \eta_{\perp}. \quad (10d)$$

The elastic discontinuity is described by η_{rs} , where $\theta(s)$ is the unit step function.

The two fields involved in the problem have different nature. The Q field has no direct conjugated physical "force" which could control its behavior, and the inclusion of gradient energy for the order parameter in the free-energy expansion renders a discontinuous space profile $Q(s)$ unstable. However, the $\tilde{\eta}$ field can be influenced by (external or internal) mechanical stress, so that discontinuous solution such as Eqs. (10a)–(10c) are possible through proper choice of defect type and distribution.

We start with Eq. (2) which gives, for the twin boundary case, rise to two coupled ordinary differential equations for Q_r and Q_s . If the coefficients were chosen to satisfy the relation

$$4A - A_n - 2\frac{\hat{B}_{22}}{\hat{c}_{22}} = 0, \quad (11)$$

Q_r and Q_s will be simply given by

$$Q_r = \frac{1}{\sqrt{2}}Q_0, \quad (12a)$$

$$Q_s = \frac{Q_0}{\sqrt{2}} \tanh\left[\frac{s}{\xi_T}\right]. \quad (12b)$$

Here ξ_T is the characteristic width of the twin boundary

$$\xi_T = (2D_{ss}/-K_s)^{1/2}, \quad (13a)$$

$$D_{ss} = \frac{1}{2}(D_{11} + D_{12}) + D_{44}, \quad (13b)$$

$$K_s = K \left[1 - \frac{1}{4A'} \left[\frac{2}{3} \frac{\hat{B}_{11}^2}{\hat{c}_{11}} + \frac{1}{3} \frac{\hat{B}_{22}^2}{\hat{c}_{22}} \right] \right]. \quad (13c)$$

The strain field given in Eqs. (10a)–(10d) satisfies the compatibility relations (5a)–(5c), so that the displacement field u can be obtained by direct integration of $\tilde{\eta}$. Nevertheless, internal body forces are needed to sustain this strain solution since the equilibrium condition, Eq. (3), is not satisfied. In order to derive the necessary forces we rewrite Eq. (3) in the following form:

$$\sigma_{ij,j}^{\text{tot}} + f_i = 0, \quad (14)$$

where f_i is the i th component of the body force density. Substituting Eqs. (10) into Eq. (14) gives

$$f_r = (B_1 - B_2) \left[\delta(s) + \frac{Q_0^2}{2\xi_T} \operatorname{sech}\left[\frac{s}{\xi_T}\right] \right], \quad (15a)$$

$$f_s = (B_1 + B_2 + B_t) \frac{Q_0^2}{\xi_T} \tanh\left[\frac{s}{\xi_T}\right] \operatorname{sech}^2\left[\frac{s}{\xi_T}\right], \quad (15b)$$

$$f_3 = 0. \quad (15c)$$

The continuous part of the force density could be realized by a suitable distribution of defects; the δ function in f_r represents an additional constant external force that must be distributed over the twin boundary plane at $s=0$. Subsequently we will refer to this solution as case I. The internal lattice displacement pattern (Q field) and the unit cell distortion ($\tilde{\eta}$ field) across the twin boundary are illustrated in Figs. 2(a) and 2(b), respectively. The solid circles in Fig. 2(a) represent the positions of the X ions in a discontinuous Q field, and the dashed circles are for the continuous solutions.¹⁴ Figures 2(b) and 2(c) are for the discontinuous and for the continuous elastic twin boundaries, respectively. Note: we have separated these two fields in order to better illustrate them; the ionic motions and the unit-cell distortions are exaggerated.

Another solution, subsequently referred to as case II, has been given in Ref. 14, which describes a twin boundary without body forces or interface defects, and for which Eqs. (2), (3), and (4) are satisfied simultaneously. But in order to sustain this solution a definite inhomogeneous stress distribution must be applied at the lateral surfaces. In other words, the lateral dimensions of the

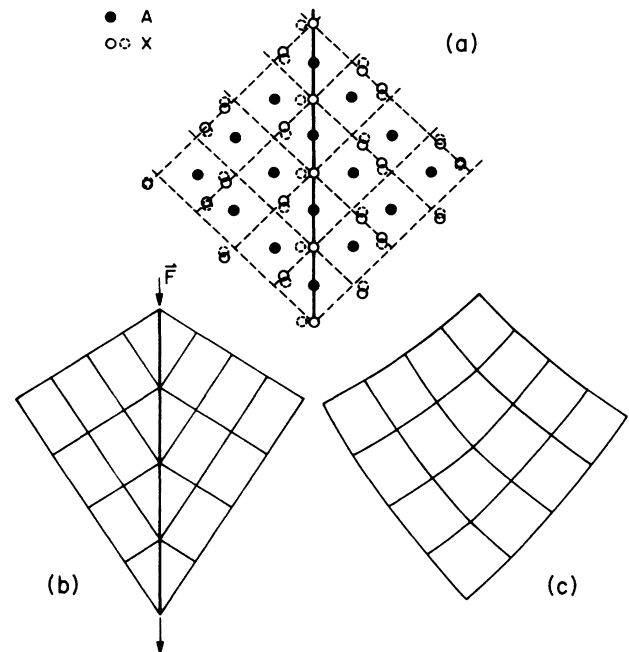


FIG. 2. Illustration of displacement and strain fields (schematic). (a) Lattice displacement pattern of X ions on plane $x_3 = a/2$ across a twin boundary (unit-cell distortion is not shown), \circ : discontinuous, dashed circle: continuous (from Ref. 14). (b) Unit-cell distortion for a twin boundary with discontinuous strain at the twin boundary. (c) Unit-cell distortion for a twin boundary with continuous strain across the twin boundary.

crystal need to be fixed while still allowing for the shape change induced by the (primary) order parameter profile. Solutions for arbitrary parameters have been given there; here we only give the closed form of $\bar{\sigma}^{\text{tot}}$ to show the characteristics of the stress distribution. With the choice of

$$4A - A_n - \left[\frac{(B_1 + B_2)^2 - B_t^2}{c_{11} + c_{12} + 2c_{44}} - \frac{2(B_1 - B_2)}{c_{11} - c_{12}} \right] = 0 \quad (16)$$

for the expansion coefficients, the total stress tensor can be written as

$$\bar{\sigma}^{\text{tot}} = \begin{pmatrix} \sigma_{rr}^{\text{tot}} & 0 & 0 \\ 0 & 0 & 0 \\ 0 & 0 & \sigma_{33}^{\text{tot}} \end{pmatrix}, \quad (17a)$$

$$\bar{\sigma}_{rr}^{\text{tot}} = \left[\frac{c_{44}}{c_{ss}} (B_1 + B_2 + B_t) - B_t \right] \frac{Q_0^2}{2} \text{sech}^2 \left[\frac{s}{\xi_T'} \right], \quad (17b)$$

$$\sigma_{33}^{\text{tot}} = \left[\frac{(c_{11} - c_{12} + 2c_{44})(B_1 + B_2 + B_t)}{4c_{ss}} - \frac{1}{2}(B_1 - B_2 + B_t) \right] \frac{Q_0^2}{2} \text{sech}^2 \left[\frac{s}{\xi_T'} \right], \quad (17c)$$

and

$$c_{ss} = \frac{1}{2}(c_{11} + c_{12} + 2c_{44}), \quad (17d)$$

$$\xi_T' = (2D_{ss} / -K_s')^{1/2}, \quad (17e)$$

$$K_s' = K \left[1 + \frac{1}{4A'} \left[\frac{2\hat{B}_{11}^2}{3\hat{c}_{33}} + \frac{\hat{B}_{33}^2}{3\hat{c}_{33}} - \frac{(B_1 + B_2)(B_1 + B_2 + B_t)}{2c_{ss}} \right] \right]. \quad (17f)$$

The lattice displacement and unit cell distortion are shown schematically in Fig. 2(a) and 2(c), respectively. We have calculated the stress components for SrTiO₃, which showed a maximum value of only -4.8×10^7 N/m² at 78 K.¹⁴

Next, we ask: what happens if one removes the body force and surface stress? Can the system still acquire a Q1D configuration without these external constraints? The answer is yes, but this case, to be referred to as III, requires the presence of a continuous distribution of dislocations. This can be seen as follows.

Under the condition that the system is stress free, i.e.,

$$\sigma_{ij}^{\text{tot}} = \frac{\partial F}{\partial \eta_{ij}} \equiv 0, \quad (ij = rr, ss, 33, rs, s3, r3). \quad (18)$$

The six independent strain components η_{ij} and the three components Q_i of the order parameter are uniquely determined by Eqs. (2) and (18). In general, this solution requires numerical integration of the set of coupled nonlinear ordinary differential equations given as Eqs. (4.40a) and (4.40b) of Ref. 14. However, an analytic solution of

the form given by Eqs. (12a) and (12b) can still be obtained for this third case if the nonlinearity parameters satisfy the condition¹⁶

$$4A - A_n = 0, \quad (19)$$

where the characteristic length for the twin boundary now becomes, instead of (13a):

$$\xi_T^* = (2D_{ss} / -K)^{1/2}. \quad (20)$$

The associated strain components for this solution are

$$\eta_{rr} = \eta_{ss} \quad (21a)$$

$$= \frac{1}{2}(\eta_{\parallel} + \eta_{\perp}) \left[1 - \frac{1}{2} \text{sech}^2(s / \xi_T^*) \right], \quad (21b)$$

$$\eta_{rs} = \frac{1}{2}(\eta_{\parallel} - \eta_{\perp}) \tanh(s / \xi_T^*), \quad (21c)$$

$$\eta_{33} = \eta_{\perp} \left[1 - \frac{1}{2} \text{sech}^2(s / \xi_T^*) \right], \quad (21d)$$

$$\eta_{s3} = \eta_{r3} = 0. \quad (21e)$$

Contrary to cases I and II the normal strain components η_{rr} and η_{33} are also functions of s (s only!), reflecting bulging or necking in the r and x_3 dimensions in the domain-wall region of the crystal. The strain solution associated with case III does not satisfy the compatibility relation (4) but instead requires the presence of a continuous distribution of dislocations [described by their density $\bar{\alpha}$ (Refs. 17 and 18)] which can be determined by the partial differential equation¹⁷

$$-\epsilon_{ikl} \epsilon_{jmn} \eta_{ln, km} = \frac{1}{2}(\epsilon_{ikl} \alpha_{lj, k} + \epsilon_{jkl} \alpha_{li, k}). \quad (22)$$

Here the right-hand side represents the ‘‘incompatibility’’ which describes the topological discontinuity introduced by the dislocations within the continuum approximation.^{17,18} Under the basic assumption Eq. (22) leads to the relations

$$\alpha_{3r} = \eta_{33, s}, \quad (23a)$$

$$\alpha_{3s} = 0, \quad (23b)$$

$$\alpha_{33} = \alpha_{rr}, \quad (23c)$$

$$\alpha_{r3} = -\eta_{rr, s}, \quad (23d)$$

$$\alpha_{rs} = 0. \quad (23e)$$

In general, $\bar{\alpha}$ can not be uniquely determined from these conditions alone. We might however assume that only bending is involved in forming a domain wall but no twisting, in other words, there are no screw dislocations at the twin boundary, so that the diagonal terms of $\bar{\alpha}$ may be set to zero.¹⁸ By inserting Eqs. (21a) and (21d) into Eqs. (23a) and (23d) we find the dislocation density for this solution to be of the form

$$\bar{\alpha} = \begin{pmatrix} 0 & 0 & \alpha_{r3} \\ 0 & 0 & 0 \\ \alpha_{3r} & 0 & 0 \end{pmatrix}, \quad (24a)$$

where

$$\alpha_{r3} = \frac{1}{2\xi_T^*} (\eta_{\parallel} + \eta_{\perp}) \operatorname{sech}^2 \left(\frac{s}{\xi_T^*} \right) \tanh \left(\frac{s}{\xi_T^*} \right), \quad (24b)$$

$$\alpha_{3r} = \frac{1}{\xi_T^*} \eta_{\perp} \operatorname{sech}^2 \left(\frac{s}{\xi_T^*} \right) \tanh \left(\frac{s}{\xi_T^*} \right). \quad (24c)$$

Equations (24) indicate that the Burgers vector for the edge dislocations introduced has only r and x_3 components and is a function of s only.

Note: here we have only considered the long-range elastic field associated with the dislocations but the "core" contributions of these defects are ignored. If one would include the "core" contributions in the energy expansion, the stable configurations might be altered.

IV. SUMMARY AND CONCLUSIONS

In this paper we have classified and derived the possible Q1D solutions for domain walls and their associated different constraints or consequences in an improper ferroelastic system. Because of the Poisson contraction in solids Q1D solutions can exist only with the presence of one of the following.

Case I. Distribution of elastic body force in the vicinity of the domain wall; for this case a sharp (discontinuous) elastic domain wall is allowed, but the order parameter changes gradually across the wall.

Case II. Distribution of surface stresses; in this case both \mathbf{Q} and $\tilde{\eta}$ fields change gradually across the domain wall, but the lateral dimensions (not the shape!) are fixed.

Case III. Continuous distribution of interface dislocations; in this case both \mathbf{Q} and $\tilde{\eta}$ fields change gradually across the domain wall, and there are no required external forces or stresses, but edge dislocations are introduced within the domain-wall region. In addition to the bending which also appears in the two previous cases, bulging or necking may occur in the lateral dimensions of the crystal near the domain wall due to the presence of these dislocations.

It is important to understand these constraints in modeling domain walls because they can introduce additional physical effects. For instance, an inhomogeneous surface stress could change the "divergence feature" of a domain wall in a first-order phase transition, which was interpreted (in Ref. 19) as a coupling effect of the order parameter to the bulk strain for a ferroelectric system. However, according to our analysis the real reason for this phenomenon is that it is due to the surface stress which

must be imposed on the system in order to support the domain-wall solution (the same as our case II). Using the method given in this paper, one can easily verify that the divergence temperature would be the same inside and outside the domain wall if interface dislocations were allowed to appear to release the surface constraints.

In conclusion, from this detailed examination of the physical requirements in obtaining a Q1D solution in a 3D improper ferroelastic system, we believe that *in the absence of external constraints a true coherent defect free planar domain-wall solution must be three dimensional (in a 3D solid)*. However, to obtain such solutions, i.e., the profiles of $\mathbf{Q}(r, s, x_3)$ and $\tilde{\eta}(r, s, x_3)$, one has to solve the fully 3D partial differential Eqs. (2)–(4), which is a mathematically challenging problem and remains to be solved.

When the domain-wall solution depends very weakly on r and x_3 , one might use an approximate method. Starting with the solution of case II as the zeroth order approximation we do the following. First, apply a new set of surface stresses to the system, which are equal in magnitude but opposite in direction to the required surface stresses in supporting the Q1D solution; this will make the system to be stress (total stress!) free. Second, solve the elasticity problem for the incremental strain $\tilde{\eta}'(r, x_3)$ with the new applied stress field. Third, use $\tilde{\eta}'(r, x_3)$ to derive from Eq. (2) the first-order correction, $\mathbf{Q}'(r, x_3)$, to the order parameter. This procedure could be iterated if needed.

In the case of SrTiO_3 numerical calculation shows that the magnitude of the required surface stress is less than $5 \times 10^7 \text{ N/m}^2$ (Ref. 14), which can produce a maximum strain value of the order of 10^{-4} . Although this strain is small compared to the elastic limit of the material, it is comparable to the transformation strain.²⁰ Therefore, it is an open question whether the above iteration technique is suitable for this material or one must develop a fully nonlinear self-consistent method. Questions of theoretical methods aside, what is clearly important physically from estimates such as this one is that surface stresses will have strong effects on domain-wall geometries.

ACKNOWLEDGMENTS

This research was supported by the U.S. Department of Energy under Grant No. DE-FG02-85ER45214 at The Pennsylvania State University, and under Grant No. DE-FG02-88ER45364 at Cornell University.

¹J. D. van der Waals, *Z. Phys. Chem.* **13**, 657 (1984).

²L. D. Landau and E. Lifshitz, *Phys. Z. Sov. Union* **8**, 153 (1935); *Electrodynamics of Continuous Media* (Pergamon, Oxford, 1960).

³L. D. Landau and L. V. Ginzburg, *J. Expt. Theor. Phys.* **20**, 1064 (1950).

⁴L. V. Ginzburg, *Nuovo Cimento* **2**, 1234 (1955).

⁵A. Hubert, *Theorie der Domänenwände in geordneten Medien* (Springer, Berlin, 1974).

⁶T. Mitsui and J. Furuchi, *Phys. Rev.* **90**, 193 (1953).

⁷V. A. Zhirnov, *Zh. Eksp. Teor. Fiz.* **35**, 1175 (1958) [*Sov.*

Phys.—*JETP* **8**, 822 (1959)].

⁸I. Ivanchik, *Fiz. Tverd. Tela* **3**, 3731 (1961) [*Sov. Phys. Solid State* **3**, 2705 (1962)].

⁹L. N. Bulaevskii, *Fiz. Tverd. Tela* **5**, 3183 (1963) [*Sov. Phys. Solid State* **5**, 2329 (1964)].

¹⁰J. W. Cahn and J. E. Hillard, *J. Chem. Phys.* **28**, 258 (1958); **30**, 1121 (1959); **31**, 688 (1959).

¹¹A. D. Bruce and R. A. Cowley, *Structural Phase Transitions* (Taylor&Francis, London, 1981).

¹²G. R. Barsch and J. A. Krumhansl, *Phys. Rev. Lett.* **54**, 1069 (1984).

¹³A. E. Jacobs, Phys. Rev. B **31**, 5984 (1985).

¹⁴W. Cao and G. R. Barsch, Phys. Rev. B **41**, 4334 (1990).

¹⁵J. C. Slonczewski and H. Thomas, Phys. Rev. B **1**, 3599 (1970).

¹⁶W. Cao, Ph.D. thesis, Pennsylvania State University, 1987.

¹⁷C. Teodosiu, *Elastic Models of Crystal Defects* (Springer, Ber-

lin, 1982).

¹⁸E. Kröner, Appl. Mech. Rev. **15**, 599 (1962).

¹⁹J. Lajzerowicz, Ferroelectrics **35**, 219 (1981).

²⁰B. Adefeld, Z. Phys. **222**, 155 (1969).